Hole-Doping Suppresses Competing Magnetism in High-DOS C136 Carbon Schwarzite: A Computational Route Toward Superconductivity in Negative-Curvature Carbon Networks

Eugene Yashin
Independent researcher, Haifa, Israel

May 12, 2026

Abstract

Carbon schwarzites are negative-curvature carbon networks whose geometry may generate electronic and lattice behavior distinct from graphene, fullerenes, and conventional carbon allotropes. Here we report a spin-polarized first-principles screening study of D-type C136 carbon schwarzite focused on the competition between magnetism, doping, and high-density-of-states metallic behavior. Neutral C136 is found to possess a robust competing magnetic branch, with total magnetization of approximately 11.01–11.03 Bohr magnetons per 136-atom cell. Charged-cell doping calculations reveal a strong electron-hole asymmetry: adding two electrons per cell increases the total magnetization to 12.11 Bohr magnetons per cell, whereas removing two electrons reduces it to 9.61 Bohr magnetons per cell. Hole doping then progressively suppresses the magnetic branch, reducing the total magnetic moment to 8.02, 6.34, and 4.76 Bohr magnetons per cell for removal of 4, 6, and 8 electrons per cell, respectively.

The most strongly hole-doped point considered here, h8, corresponding to removal of eight electrons per 136-atom cell, was further examined using spin-polarized NSCF and density-of-states calculations on a $4 \times 4 \times 4$ k-point mesh. The NSCF Fermi energy, -0.7414 eV, agrees with the SCF value of -0.7413 eV. The spin-resolved DOS shows that high-DOS metallic character is retained near the Fermi level: at $E = -0.740$ eV, the total DOS is approximately 44.69 states/eV/cell, with $\mathrm{DOS}_\uparrow = 33.11$ and $\mathrm{DOS}_\downarrow = 11.58$ states/eV/cell. Thus h8 combines substantial suppression of the competing magnetic branch with preservation of a high-DOS Fermi-level environment.

We do not claim superconductivity in C136. Rather, these calculations identify hole doping as a concrete route for suppressing a competing magnetic instability while preserving the electronic conditions required for further superconductivity screening. A preliminary Gamma-point phonon pilot indicates that full lattice-stability and electron-phonon calculations are computationally demanding for this 136-atom charged spin-polarized system. Lattice stability, electron-phonon coupling, and superconducting transition-temperature estimates therefore remain open problems for subsequent work.

1 Introduction

Carbon-based materials have repeatedly served as model systems for exploring how geometry, dimensionality, and electronic structure interact. Graphene, fullerenes, nanotubes, and doped covalent carbon networks demonstrate that the same element can support radically different electronic behavior depending on bonding topology and curvature. Carbon schwarzites extend this landscape to triply periodic, negative-curvature frameworks [1]. Related triply periodic minimal surface graphene foams have also been studied as three-dimensional carbon networks

with unusual mechanical and geometric properties [2]. Unlike fullerenes, where positive curvature closes the carbon network into cages, schwarzites are open three-dimensional networks related to triply periodic minimal surfaces. This makes them attractive as theoretical platforms for studying how negative Gaussian curvature, extended π bonding, and three-dimensional connectivity reshape the electronic density of states near the Fermi level.

The possible connection between unusual carbon network geometry and superconductivity is especially intriguing. In conventional electron-phonon superconductivity, a high density of states at the Fermi level can enhance pairing tendencies, provided that lattice stability and electron-phonon coupling are favorable [9, 10]. However, high-DOS electronic structures are often accompanied by competing instabilities. These may include spin polarization, charge ordering, Peierls-like distortions, or soft lattice modes. Therefore, the presence of a high DOS alone is not sufficient evidence for superconductivity. A credible superconductivity search must also identify and characterize the instabilities that compete with pairing.

In the present work we focus on D-type C136 carbon schwarzite as a candidate negative-curvature carbon framework. This work follows a previous spin-polarized study of D-type C136 carbon schwarzite, where a framework-preserving high-DOS state and competing spin/lattice instabilities were identified [3]. The present article narrows the question further. Rather than asking whether C136 is already superconducting, we ask a more basic screening question: can charged-cell hole doping suppress the competing magnetic branch while preserving high-DOS metallic character near the Fermi level?

To answer this question, we performed spin-polarized first-principles calculations using Quantum ESPRESSO [7, 8]. We first examined the magnetic behavior of neutral C136 and found that it possesses a robust spin-polarized branch with a total magnetization of approximately 11.01–11.03 Bohr magnetons per 136-atom cell. This result implies that neutral C136 is not simply a non-magnetic high-DOS metal; instead, magnetism is a serious competing instability. We then carried out a charged-cell doping screen to test how the magnetic branch responds to electron and hole doping.

The results reveal a clear electron-hole asymmetry. Adding two electrons per cell strengthens the magnetic branch, increasing the total magnetization to 12.11 Bohr magnetons per cell, whereas removing two electrons reduces it to 9.61 Bohr magnetons per cell. In the hole-doped series, the total magnetic moment then decreases monotonically to 8.02, 6.34, and 4.76 Bohr magnetons per cell for removal of 4, 6, and 8 electrons per cell, respectively. The h8 point, corresponding to removal of eight electrons per 136-atom cell, gives the strongest magnetic suppression observed in the present screen.

The key issue is whether this magnetic suppression destroys the high-DOS electronic state. To test this, we performed spin-polarized NSCF and density-of-states calculations for h8 on a $4\times 4\times 4$ k-point mesh. The h8 state remains metallic and high-DOS near the Fermi level, with total DOS near E_F of approximately 44.69 states/eV/cell. Thus h8 combines reduced magnetism with preserved high-DOS metallic character, making it the strongest current candidate point for further superconductivity screening in this structure.

However, this work does not demonstrate superconductivity. Lattice stability and electron-phonon coupling remain unresolved. A preliminary Gamma-point phonon pilot for h8 showed that direct phonon calculations are computationally demanding for this charged, spin-polarized 136-atom cell. Existing finite-displacement phonopy data for related C136 calculations contain 78 displacement structures, indicating that full phonon and electron-phonon calculations require substantial computational resources. We therefore frame the present work as a cost-aware screening study: it identifies a promising hole-doped electronic regime, while clearly separating this result from the still-open tasks of lattice-stability verification and electron-phonon superconductivity analysis.

2 Computational Methods

All first-principles calculations were performed within density-functional theory using Quantum ESPRESSO [7, 8]. The calculations used the PBE exchange-correlation functional [4] and a carbon PAW pseudopotential, `C.pbe-n-kjpaw_psl.1.0.0.UPF`, from PSLibrary [6]. Plane-wave kinetic-energy cutoffs were set to `ecutwfc = 40 Ry` and `ecutrho = 320 Ry`. Electronic occupations were treated with Marzari–Vanderbilt smearing [5], using `degauss = 0.01 Ry`. Spin-polarized calculations were performed with `nspin = 2`.

The structural model considered here is a 136-atom D-type carbon schwarzite cell. The calculations used a cell representation with `ibrav = 0`, `nat = 136`, and `ntyp = 1`. The same atomic structure and computational settings were used throughout the charged-cell doping screen unless otherwise stated. Symmetry was disabled using `nosym = .true.` and `noinv = .true.` in order to avoid imposing symmetry constraints on the spin-polarized solutions. This is important for the present screening because symmetry operations can otherwise artificially constrain local spin polarization and make competing magnetic branches harder to detect.

For the neutral magnetic tests and charged-cell doping screen, self-consistent-field calculations were performed with a $3\times3\times3$ automatic k-point mesh. The electronic convergence threshold was set to `conv_thr = 1.0d-6`, with `electron_maxstep = 100`. The starting magnetization was set to `starting_magnetization(1) = 0.1` for the main spin-polarized magnetic branch calculations. A weak-seed nearly non-magnetic calculation with `starting_magnetization(1) = 0.001` was also used to test whether a low-magnetization branch could be obtained.

Charged-cell doping was modeled using the Quantum ESPRESSO `tot_charge` parameter. Positive `tot_charge` corresponds to removal of electrons from the simulation cell, i.e. hole doping, while negative `tot_charge` corresponds to electron doping. The charged-cell states considered in this work are listed in Table 1.

Table 1: Charged-cell states considered in the C136 doping screen.

Label	Electron-count change	QE `tot_charge`
Neutral	0	0
e2	+2 electrons/cell	-2
h2	-2 electrons/cell	+2
h4	-4 electrons/cell	+4
h6	-6 electrons/cell	+6
h8	-8 electrons/cell	+8

Because periodic charged-cell calculations use a compensating background charge, total energies from different charge states were not used as the primary comparison metric. The primary screening diagnostic was the spin-polarized magnetic moment, especially the total magnetization and absolute magnetization reported by Quantum ESPRESSO. This choice was made because the objective of the screen was to identify whether electron or hole doping suppresses the competing magnetic branch.

For the h8 state, an additional non-self-consistent calculation was performed using the converged h8 spin-polarized SCF state as input. The NSCF calculation used a $4\times4\times4$ k-point mesh, `restart_mode = 'restart'`, `startingpot = 'file'`, and `startingwfc = 'file'`, with the same prefix and output directory as the converged h8 SCF calculation. The NSCF Fermi energy was compared with the SCF Fermi energy as a consistency check.

The density of states for h8 was calculated using `dos.x` from the h8 NSCF result. The DOS calculation used the energy window `Emin = -5.0 eV`, `Emax = 5.0 eV`, and `DeltaE = 0.01 eV`. The resulting DOS file reports a Fermi energy of `EFermi = -0.741 eV`. Spin-resolved DOS values were analyzed around the Fermi level by summing the spin-up and spin-down components.

A preliminary Gamma-point phonon pilot was attempted for the h8 state using `ph.x`. This was not intended as a full phonon calculation. Only representation 1 was requested using `start_irr = 1` and `last_irr = 1`, with `search_sym = .false.` and `recover = .false.`. The calculation successfully read the h8 save directory and constructed the Gamma-point perturbation list, generating 408 representations. Representation 1 was marked as `To be done`, and representations 2–408 were marked as `Not done in this run`. However, the output stopped growing after the line `Compute atoms: 1,`, and the job was manually stopped to avoid unnecessary computational expense. Therefore no phonon frequencies are reported in the present work.

Existing finite-displacement phonopy files for the related C136 setup were also inspected to estimate computational scale. The file `phonopy_disp.yaml` contained 78 displacement entries, and the directory `phonopy_fd/inputs` contained 78 corresponding `phonopy_*.in` files. This indicates that a full finite-displacement phonon calculation for this 136-atom cell would require 78 separate SCF force calculations in the existing setup. Full phonon spectra and electron-phonon coupling calculations were therefore deferred to future work.

3 Results

3.1 Neutral C136 has a competing magnetic branch

The first step was to determine whether neutral C136 behaves as a simple non-magnetic high-DOS metal or whether spin polarization produces a competing magnetic state. This distinction is essential for any superconductivity-oriented screening study, because a high density of states at the Fermi level can enhance not only pairing tendencies but also magnetic instabilities.

Spin-polarized SCF calculations show that neutral C136 supports a robust magnetic branch. For the representative magnetic solution, the total magnetization is approximately 11.01–11.03 Bohr magnetons per 136-atom cell, while the absolute magnetization is approximately 12.15–12.16 Bohr magnetons per cell. These values are large on the scale of a carbon-only unit cell and indicate that the neutral high-DOS electronic structure is strongly susceptible to spin polarization.

A weak-seed calculation was also used to test whether a nearly non-magnetic branch could be obtained. With a very small starting magnetization, the calculation produced a low-magnetization solution with total magnetization of approximately 0.10 Bohr magnetons per cell and absolute magnetization of approximately 0.20 Bohr magnetons per cell. However, this weakly magnetic solution is not the representative magnetic branch. The spin-polarized magnetic branch is lower in total energy by approximately 0.037 Ry, corresponding to about 0.50 eV per 136-atom cell. The weak-seed solution should therefore be interpreted as a metastable or higher-energy SCF branch rather than as the ground-state reference.

This result changes the interpretation of neutral C136. The material should not be described simply as a non-magnetic high-DOS metal. Rather, the neutral system contains a strong competing magnetic instability. In the context of superconductivity screening, this magnetic branch is a competing order that must be suppressed or bypassed before electron-phonon superconductivity can be meaningfully assessed.

3.2 Charged-cell doping screen: electron-hole asymmetry

Having established that neutral C136 possesses a strong competing magnetic branch, we next tested whether doping can suppress this instability. Charged-cell calculations were performed using the Quantum ESPRESSO `tot_charge` parameter. In this convention, positive `tot_charge` removes electrons from the cell and models hole doping, while negative `tot_charge` adds electrons and models electron doping.

The first comparison reveals a clear electron-hole asymmetry. Adding two electrons per 136-atom cell increases the total magnetization to 12.11 Bohr magnetons per cell and the absolute magnetization to 12.88 Bohr magnetons per cell. Thus, electron doping does not suppress the magnetic branch in this structure; instead, it strengthens it relative to neutral C136.

Hole doping has the opposite effect. Removing two electrons per cell reduces the total magnetization to 9.61 Bohr magnetons per cell and the absolute magnetization to 11.13 Bohr magnetons per cell. This already indicates that the hole-doped side is the more promising direction for bypassing the competing magnetic instability.

The contrast between the +2-electron and -2-electron cases is important because it shows that the response is not simply a generic effect of changing the electron count. The magnetic branch is sensitive to the direction of Fermi-level shift: electron doping strengthens spin polarization, whereas hole doping weakens it.

3.3 Hole doping monotonically suppresses the competing magnetic branch

The hole-doping series shows a monotonic suppression of the competing magnetic branch. Starting from the neutral magnetic solution with total magnetization of approximately 11.0 Bohr magnetons per 136-atom cell, removal of electrons progressively reduces the total magnetic moment. Removing two electrons per cell gives $M_{\mathrm{tot}} = 9.61$ Bohr magnetons per cell, removing four electrons gives $M_{\mathrm{tot}} = 8.02$, removing six electrons gives $M_{\mathrm{tot}} = 6.34$, and removing eight electrons gives $M_{\mathrm{tot}} = 4.76$. The absolute magnetization follows the same overall trend, decreasing from approximately 12.15–12.16 Bohr magnetons per cell in neutral C136 to 7.21 Bohr magnetons per cell in the h8 state.

This trend is summarized in Figure 1. The monotonic reduction of both total and absolute magnetization indicates that hole doping does not merely change the sign or distribution of local magnetic moments; it systematically weakens the spin-polarized branch. Among the charge states considered here, h8 is the most effective point for suppressing magnetism.

This result identifies hole doping as a concrete route for moving C136 away from the magnetic instability that dominates the neutral high-DOS state. However, magnetic suppression alone is not sufficient for superconductivity screening. A useful candidate must also retain metallic or high-DOS electronic structure near the Fermi level. The h8 state was therefore selected for a more detailed NSCF and density-of-states analysis.

3.4 h8 preserves high-DOS metallic character near EF

The h8 state gives the strongest suppression of the magnetic branch in the present charged-cell screen. The next question is whether this magnetic suppression is achieved at the cost of destroying the metallic high-DOS electronic structure. To test this, we performed a spin-polarized NSCF calculation for h8 using a $4 \times 4 \times 4$ k-point mesh, followed by a spin-resolved density-of-states calculation.

The NSCF calculation is consistent with the converged h8 SCF state. The Fermi energy from the NSCF calculation is -0.7414 eV, in close agreement with the SCF Fermi energy of -0.7413 eV. The DOS file reports EFermi $= -0.741$ eV. This agreement indicates that the NSCF calculation is sampling the same electronic state obtained in the h8 SCF calculation.

The resulting spin-resolved DOS shows that h8 remains metallic and high-DOS near the Fermi level. At $E = -0.740$ eV, the nearest DOS grid point to $E_F = -0.741$ eV, the spin-up DOS is 33.11 states/eV/cell and the spin-down DOS is 11.58 states/eV/cell, giving a total DOS of 44.69 states/eV/cell. Across the window $E_F \pm 0.05$ eV, the total DOS remains high, approximately in the range 35.4–48.4 states/eV/cell.

This is the central electronic result of the present work. Hole doping to h8 substantially weakens the competing magnetic branch, reducing the total magnetic moment from approximately 11.0 to 4.76 Bohr magnetons per cell, but it does not eliminate the high-DOS metallic

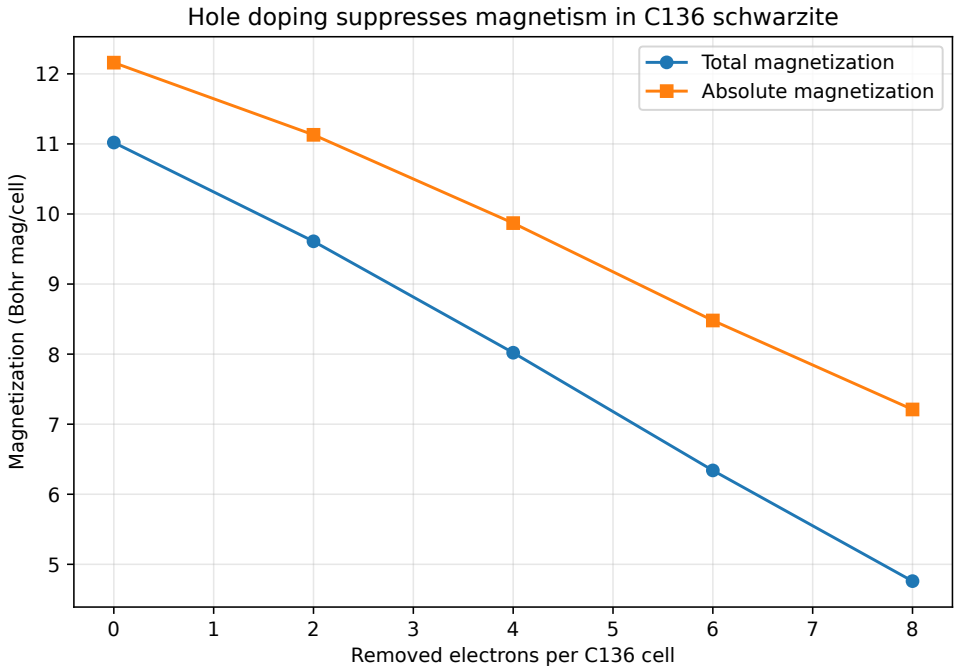

Figure 1: Hole-doping suppression of the competing magnetic branch in C136 carbon schwarzite. The plot shows total and absolute magnetization as a function of removed electrons per 136-atom cell. Hole doping monotonically reduces the total magnetic moment from approximately 11.0 Bohr magnetons per cell in neutral C136 to 4.76 Bohr magnetons per cell for h8, corresponding to removal of eight electrons per cell.

environment near the Fermi level. At the same time, h8 is not a non-magnetic metal: the Fermi-level DOS remains strongly spin-polarized, with a spin-up to spin-down DOS ratio of approximately 2.86 at the nearest DOS grid point to E_F. Instead, h8 combines reduced magnetism with a spin-polarized high-DOS metallic state at E_F. This combination makes h8 the strongest current candidate point for subsequent superconductivity screening in C136.

Figure 2 shows the spin-resolved DOS for h8. The wide panel places the Fermi-level region in the broader DOS context, while the zoom panel highlights the high-DOS behavior directly around E_F. The vertical dashed line marks E_F.

3.5 Lattice-stability bottleneck and phonon cost

Although h8 is the most promising electronic point found in the present screen, superconductivity cannot be claimed from magnetic suppression and high DOS alone. A physically meaningful superconductivity candidate must also be lattice-stable, or at least must relax into a nearby distorted structure that preserves the relevant metallic high-DOS electronic character. For this reason, the next natural step is a phonon or lattice-stability analysis.

A preliminary Gamma-point phonon pilot was attempted for h8 using `ph.x`. The calculation was deliberately restricted to a single irreducible representation, with `start_irr = 1` and `last_irr = 1`, in order to test the feasibility of the calculation before committing to a full phonon run. The calculation successfully read the converged h8 save directory and constructed the Gamma-point perturbation list. Because symmetry reduction was effectively absent under the chosen settings, `ph.x` generated 408 representations, corresponding to the 3×136 atomic degrees of freedom. Representation 1 was marked as `To be done`, while representations 2–408 were marked as `Not done in this run`, confirming that the restriction to one representation worked as intended.

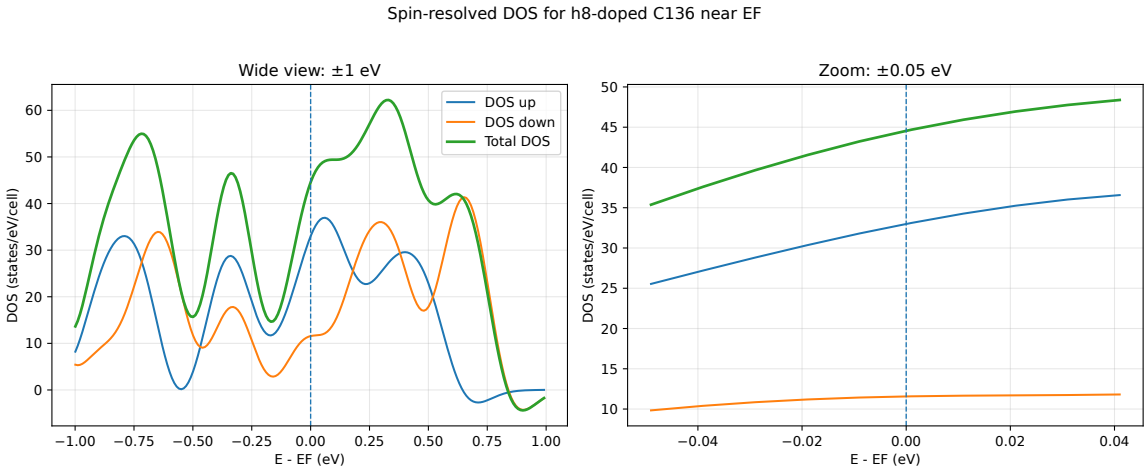

Figure 2: Spin-resolved density of states for h8-doped C136 carbon schwarzite. The h8 state corresponds to removal of eight electrons per 136-atom cell, modeled with QE `tot_charge = +8`. The vertical dashed line marks the Fermi level. The left panel shows the DOS in a ± 1 eV window around E_F, while the right panel zooms into the $E_F \pm 0.05$ eV region. At $E = -0.740$ eV, the nearest DOS grid point to $E_F = -0.741$ eV for the 0.01 eV DOS mesh, the spin-up DOS is 33.11 states/eV/cell and the spin-down DOS is 11.58 states/eV/cell, giving $\mathrm{DOS}_{\mathrm{total}} \approx 44.69$ states/eV/cell.

However, the output stopped growing after the line `Compute atoms: 1,`, and the job continued to consume CPU time without producing further useful output. The run was therefore stopped manually. No phonon frequencies were obtained from this pilot calculation. This result does not establish a lattice instability, but it does show that direct DFPT phonon calculations for the charged, spin-polarized h8 state are computationally demanding under the present settings. This behavior is consistent with the cost of entering the first linear-response perturbation for a charged spin-polarized 136-atom cell with disabled symmetry. In such a calculation, the Sternheimer response must be solved over a large Bloch-state manifold, and the absence of symmetry reduction leaves the full set of $3N$ atomic perturbations to be considered.

The finite-displacement route is also computationally demanding. Existing phonopy files for the related C136 setup were inspected to estimate the scale of a full finite-displacement calculation. The file `phonopy_disp.yaml` contains 78 displacement entries, and the directory `phonopy_fd/inputs` contains 78 corresponding `phonopy_*.in` files. Thus, in the existing setup, a full finite-displacement phonon calculation would require 78 separate SCF force calculations.

The present work therefore treats lattice stability as an unresolved bottleneck rather than as a solved problem. The appropriate next step is a cost-aware lattice sanity strategy: for example, a displacement-count test for any modified setup, one or a few frozen-displacement SCF tests, or a symmetry/cost-reduction strategy before attempting full phonons. Only if the lattice response is acceptable should full phonon spectra and electron-phonon coupling calculations be pursued.

4 Limitations

The present work should be understood as a computational screening study rather than as a demonstration of superconductivity in C136. Several limitations are important.

First, the charged-cell calculations use the Quantum ESPRESSO `tot_charge` parameter and therefore include a compensating background charge. Such calculations are useful for screening the response of the electronic structure to electron-count changes, but total energies from different charge states should not be interpreted as directly comparable formation energies.

In the present work, the charged-cell calculations are used primarily to track the evolution of spin polarization with electron and hole doping.

Second, lattice stability of the h8 state has not been established. The h8 point is electronically promising because it combines reduced magnetism with high DOS near E_F, but this does not guarantee that the corresponding lattice configuration is dynamically stable. A preliminary Gamma-point phonon pilot was attempted, but no phonon frequencies were obtained. Therefore, imaginary modes, soft distortions, or structural instabilities cannot be excluded.

Third, electron-phonon coupling has not been calculated. No values of λ, $\omega_{\log}$, $\alpha^2F(\omega)$, or superconducting transition temperature are reported here. Consequently, the present work does not claim that h8-doped C136 is superconducting. It identifies h8 as a candidate point for further superconductivity screening.

Fourth, the h8 charge state is a model of hole doping rather than a specific experimentally realized chemical composition. Removal of eight electrons from a 136-atom cell corresponds to approximately 0.059 holes per carbon atom, or about 5.9% hole doping on a per-atom basis. This scale is not obviously outside the broad range encountered in doped carbon materials, including boron-doped diamond and graphite intercalation compounds [11, 12]; however, an explicit chemical realization may require substitutional dopants, electrostatic gating, charge transfer from intercalants, or another doping mechanism. Such realization may modify the structure, symmetry, lattice stability, and electronic structure.

Fifth, the present magnetic screen used a single carbon atomic type and a ferromagnetic-like starting magnetization. Antiferromagnetic, ferrimagnetic, non-collinear, or more complex local-moment patterns were not exhaustively tested. Therefore, the reported magnetic solution should be interpreted as a robust competing spin-polarized branch rather than as definitive identification of the global magnetic ground state across all possible magnetic orderings.

Finally, the DOS calculations reported here are screening-level calculations. The h8 DOS was obtained from a $4 \times 4 \times 4$ NSCF mesh. This is sufficient to identify high-DOS metallic character near E_F, but future work should test convergence with respect to k-point density, smearing, structural relaxation, and possible distorted configurations.

Taken together, these limitations define the next stage of the research program: determine whether the h8 electronic state is lattice-stable or whether it relaxes into a nearby distorted structure, and only then proceed to full phonon and electron-phonon coupling calculations.

5 Conclusions

We have performed a spin-polarized first-principles screening study of D-type C136 carbon schwarzite focused on the competition between magnetism, doping, and high-DOS metallic behavior. Neutral C136 is found to possess a robust competing magnetic branch with total magnetization of approximately 11.01–11.03 Bohr magnetons per 136-atom cell. Electron doping strengthens this magnetic branch, increasing M_{tot} to 12.11 Bohr magnetons per cell for e2, whereas hole doping progressively suppresses it.

The hole-doped series shows a monotonic decrease in total magnetization from approximately 11.0 Bohr magnetons per cell in neutral C136 to 9.61, 8.02, 6.34, and 4.76 Bohr magnetons per cell for removal of 2, 4, 6, and 8 electrons per cell, respectively. The h8 state is therefore the most magnetically suppressed point in the present screen.

A spin-polarized NSCF/DOS calculation shows that h8 retains high-DOS metallic character near the Fermi level. At $E = -0.740$ eV, close to $E_F = -0.741$ eV, the spin-up and spin-down DOS values are 33.11 and 11.58 states/eV/cell, giving $\mathrm{DOS}_{\mathrm{total}} \approx 44.69$ states/eV/cell. Thus h8 combines reduced magnetism with preservation of a high-DOS Fermi-level environment.

We do not claim superconductivity in C136. Instead, the result identifies hole doping as a concrete route for suppressing competing magnetism while retaining the electronic conditions that motivate further superconductivity screening. Lattice stability and electron-phonon cou-

pling remain open problems. The next step is a cost-aware lattice-stability strategy, followed by full phonon and EPC calculations only if the lattice response is favorable.

AI-assisted writing and analysis disclosure

The author used large language models, including ChatGPT, Claude, and Gemini, as assistive tools for planning calculations, interpreting output logs, drafting command-line workflows, organizing results, and editing manuscript text. All numerical results were generated using Quantum ESPRESSO and related scientific software. The author reviewed and approved the final manuscript and remains responsible for its scientific content.

References

[1] A. L. Mackay and H. Terrones, "Diamond from graphite," *Nature* **352**, 762 (1991). doi:10.1038/352762a0.

[2] G. S. Jung and M. J. Buehler, "Multiscale Mechanics of Triply Periodic Minimal Surfaces of Three-Dimensional Graphene Foams," *Nano Letters* **18**, 4845–4853 (2018). doi:10.1021/acs.nanolett.8b01431.

[3] E. Yashin, "Ab initio evidence for a framework-preserving spin-polarized high-DOS state in D-type carbon schwarzite C136," arXiv:2605.02082 [cond-mat.mtrl-sci] (2026).

[4] J. P. Perdew, K. Burke, and M. Ernzerhof, "Generalized Gradient Approximation Made Simple," *Physical Review Letters* **77**, 3865–3868 (1996). doi:10.1103/PhysRevLett.77.3865.

[5] N. Marzari, D. Vanderbilt, A. De Vita, and M. C. Payne, "Thermal Contraction and Disordering of the Al(110) Surface," *Physical Review Letters* **82**, 3296–3299 (1999). doi:10.1103/PhysRevLett.82.3296.

[6] A. Dal Corso, "Pseudopotentials periodic table: From H to Pu," *Computational Materials Science* **95**, 337–350 (2014). doi:10.1016/j.commatsci.2014.07.043.

[7] P. Giannozzi *et al.*, "QUANTUM ESPRESSO: a modular and open-source software project for quantum simulations of materials," *Journal of Physics: Condensed Matter* **21**, 395502 (2009). doi:10.1088/0953-8984/21/39/395502.

[8] P. Giannozzi *et al.*, "Advanced capabilities for materials modelling with Quantum ESPRESSO," *Journal of Physics: Condensed Matter* **29**, 465901 (2017). doi:10.1088/1361-648X/aa8f79.

[9] W. L. McMillan, "Transition Temperature of Strong-Coupled Superconductors," *Physical Review* **167**, 331–344 (1968). doi:10.1103/PhysRev.167.331.

[10] P. B. Allen and R. C. Dynes, "Transition temperature of strong-coupled superconductors reanalyzed," *Physical Review B* **12**, 905–922 (1975). doi:10.1103/PhysRevB.12.905.

[11] E. A. Ekimov, V. A. Sidorov, E. D. Bauer, N. N. Mel'nik, N. J. Curro, J. D. Thompson, and S. M. Stishov, "Superconductivity in diamond," *Nature* **428**, 542–545 (2004). doi:10.1038/nature02449.

[12] T. E. Weller, M. Ellerby, S. S. Saxena, R. P. Smith, and N. T. Skipper, "Superconductivity in the intercalated graphite compounds C6Yb and C6Ca," *Nature Physics* **1**, 39–41 (2005). doi:10.1038/nphys0010.